

Fig. 7. Variation with west longitude of the escape speed for clasts projected horizontally to the east from the vicinity of the east rim of Stickney at 30°W.

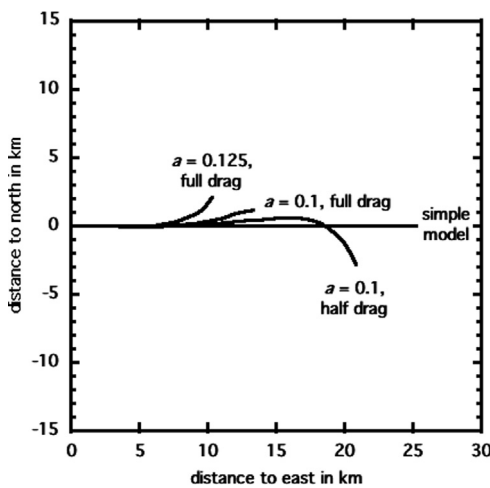


Fig. 8. Calculated tracks of 250 m-radius boulders ejected horizontally along the equator from a starting point at the approximate location of Stickney's east rim, longitude 30°W, at an initial speed of 5.0 m s^{-1} , for three combinations of the groove profile parameter, a , and the amount of regolith friction drag force assumed.

increases the eastward travel distance to $\sim 13.3 \text{ km}$. The longest path shown, with an eastward distance of $\sim 21 \text{ km}$, corresponds to decreasing the drag force by a factor of 2 to simulate a boulder that bounces along part of its horizontal traverse. As might be expected, decreasing the frictional force allows the boulder to respond to a greater extent to the gravitational slope in the north–south direction. For the shorter travel distances (i.e., $\sim 10.3 \text{ km}$ and $\sim 13.3 \text{ km}$), this causes the boulder to deviate to the north, but for the greatest travel distance ($\sim 21 \text{ km}$) a southward slope is eventually encountered and this dominates the terminal stages of its motion, causing a final southward displacement of $\sim 2.8 \text{ km}$. Note that these values of north- and southward displacement are illustrative rather than definitive, because we did not take detailed account of the surface topography more than 2° of latitude on either side of the equator; nevertheless, these results indicate the trends that would be shown by a more detailed analysis. The horizontal line shown in Fig. 8, extending eastward to $\sim 25 \text{ km}$, is the result of using $a=0.1$ and adopting the local values of g but ignoring the variations of actual topography and gravitational potential topography. Its greater extent, relative to the corresponding detailed model, shows that the simple model of Section 4 (which neglects topography) overestimates boulder travel distances in this region of Phobos' surface by $\sim 20\%$.

We are now able to appraise the scenario under which boulders are not seen at the ends of grooves because they reach the local

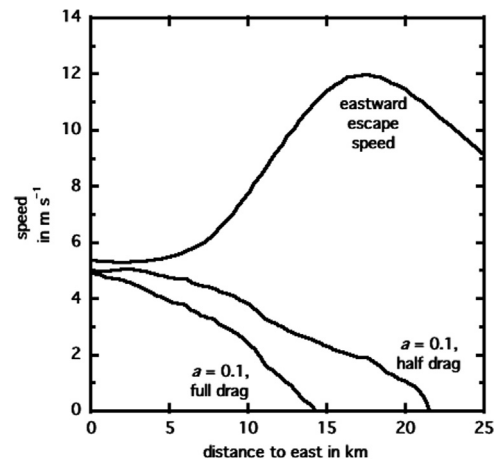


Fig. 9. Speed of a 250 m-radius boulder as a function of eastward distance traveled from the vicinity of Stickney for $a=0.1$ and for either 100% or 50% of the drag force given by Eq. (5). Also shown for comparison is the variation of eastward escape speed along the boulder tracks.

escape velocity after rolling or bouncing for some distance across the surface. Fig. 9 illustrates the speed as a function of eastward distance traveled for two of the three cases shown in Fig. 8 for a 250 m radius boulder. Here, $a=0.1$ where the full drag force is applied, and $a=0.1$ where half the drag force is applied. The variation of eastward escape speed along the boulder tracks is also shown. The region from 0 to 7.5 km shows how local topography can influence the speed of a boulder. For example, at ~ 2.5 and $\sim 6 \text{ km}$ along the track, an increase in speed due to favorable topography reverses the general deceleration of the boulder due to regolith friction. However, it is also clear that unless the initial speed of the boulder is close to the escape speed at the location from which it is launched, it will not attain escape velocity anywhere along its track.

Given the delicate balance implied by Fig. 9 between the forces controlling whether boulders can escape after forming a groove, we have explored the relationships between the influences of boulder size, regolith friction, and initial speed. Fig. 10 shows the control of regolith friction for a fixed boulder radius of 250 m. Fig. 10a–c shows the variation of speed with distance traveled when the regolith friction is 100%, 50%, and 25%, respectively, of the amount implied by Eq. (5). With full friction (Fig. 10a), the speeds of all boulders decrease monotonically over the first few km and boulders either have escape speed at the instant they begin to move or they never reach escape velocity; all those launched at speeds greater than 5.37 m s^{-1} escape immediately. For friction at an assumed 50% (Fig. 10b), all boulders launched at greater than 5.37 m s^{-1} again escape immediately. A boulder launched at 5.30 m s^{-1} initially slows down as it forms a groove but then speeds up until it just attains escape velocity after traveling almost exactly 2 km. All boulders launched at speeds between 5.30 and 5.37 m s^{-1} escape after forming grooves that extend some distance less than 2 km, and all boulders launched at speeds below 5.30 m s^{-1} form much longer grooves but never escape. With friction at 25% applied (Fig. 10c), all boulders launched with speeds between 5.00 and 5.37 m s^{-1} escape after forming grooves up to 3 km in length, and it is only boulders launched at speeds less than 5.00 m s^{-1} that remain present at the end of the groove (having formed much longer grooves).

Fig. 11 shows the importance of boulder size for a fixed value of the friction. To find the most favorable cases we assume that 25% of the friction implied by Eq. (5) acts on the boulder. Fig. 11a–c shows the speed–distance relationship for boulders with radii of 50, 150, and 250 m, respectively. Fig. 11c is thus identical to